Current Physical Chemistry, **2017**, *7*, **000-000**

REVIEW ARTICLE

A Review Article about the Deactivation of Poly(o-aminophenol) film Electrodes Employing Impedance Spectroscopy and Surface Resistance

Ricardo I. Tucceri*

Instituto de Investigaciones Fisicoquímicas Teóricas y Aplicadas (INIFTA), CONICET, Facultad de Ciencias Exactas, Universidad Nacional de La Plata, Sucursal 4, Casilla de Correo 16, (1900) La Plata, Argentina

ARTICLE HISTORY

Received: April 20, 2017
Revised: May 10, 2017
Accepted: July 28, 2017

DOI:
10.2174/1877946807666170807154749

Abstract: ***Objective:*** Storage time without use (STWU) in the supporting electrolyte solution for time periods beyond 30 hours deactivates poly(o-aminophenol) (POAP) films.

Observations: Deactivated POAP films exhibit a lower conductivity than freshly prepared (nondeactivated) films Considering the interest in POAP synthesized in acid medium in both basic and applied research, not much attention has been paid to the decay of the electroactivity of POAP caused by its extensive use.

Conclusion: Deactivation of poly(o-aminophenol) (POAP) film electrodes by STWU in the supporting electrolyte solution is reviewed in this work

Keywords: Deactivation of poly(o-aminophenol), conductivity, charge transport parameters, surface resistance, steady-state, diffusion coefficient.

1. INTRODUCTION

Different sensors based on the good conductivity of POAP have been reported in the literature [1-4]. These sensors are employed in different analytical determinations [2, 3] after being stored for long time periods in the working solution. However, a loss of conductivity was observed as the storage time of POAP was extended beyond 30 h. The loss of conductivity of POAP was studied in our laboratory by employing different electrochemical techniques [5-7]. Results about POAP deactivation are reviewed here.

2. CYCLIC VOLTAMMETRY STUDIES

The voltammetric response corresponding to a nondeactivated (immediately prepared) POAP film is shown in Fig. **1** (plot (a)). The POAP film maintains this response within the potential range $-0.2\text{ V} < E < 0.5\text{ V}$ even after being stored without use in the supporting electrolyte solution for 32 h. However, after a higher storage time, this response dramatically changes. In Fig. **1** the *j-E* response of a nondeactivated POAP film (plots (a)) is compared with that of the films (see first column of Table **1**) that were stored without use in the supporting electrolyte for the time periods listed in column 2 of Table **1**.

The more attenuated voltammetric response is observed in Fig. **1**, as the increasing storage time indicates a deactivation of the POAP film. In this regard, voltammetric reduction charge values corresponding to the completely reduced POAP films were compared for a nondeactivated film ($Q_{\mathrm{Red,T}}$ = 2.8 mC cm^{-2}) and the different deactivated films ($Q_{\mathrm{Red,c}}$) indicated in Table **1**. Then, a degree of deactivation (column 4 of Table **1**) was defined as

$$\theta_c^{d} = 1 - (Q_{\mathrm{Red,c}}/Q_{\mathrm{Red,T}}) \qquad (1)$$

$Q_{\mathrm{Red,c}}$ is the total reduction charge assessed by integration of the corresponding *j-E* response from E = 0.5 V towards the negative potential direction for a deactivated film, and $Q_{\mathrm{Red,T}}$ = 2.8 mC cm^{-2} is the total reduction charge for the nondeactivated film.

---

*Address correspondence to this author at the Instituto de Investigaciones Fisicoquímicas Teóricas y Aplicadas (INIFTA), Sucursal 4, Casilla de Correo 16, (1900) La Plata, Argentina; Fax: (54) (0221) 425-4642; E-mail: rtucce@inifta.unlp.edu.ar

1877-9468/17 $ 58.00+.00

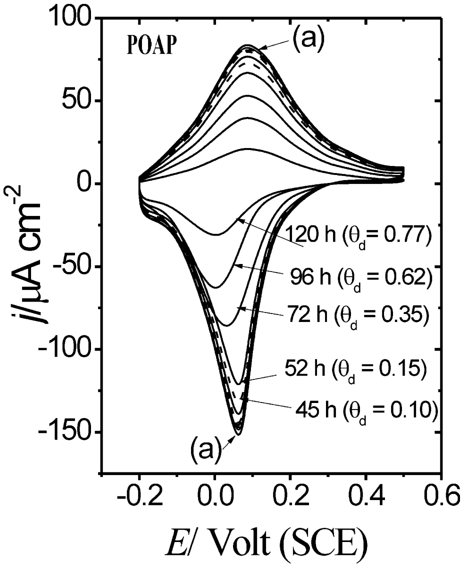

Fig. (1). Voltammetric (j-E) responses of a POAP film (thickness: ϕ_p = 60 nm, voltammetry charge: 2.8 mC cm^{-2}). (a) A nondeactivated POAP film. The other voltammetric responses correspond to POAP films which were held without use in the supporting electrolyte solution for the time periods indicated in the figure. The degrees of deactivation (θ_d) of the films are indicated in Table **1**. Electrolyte: 0.1 M $HClO_4$ + 0.4 M $NaClO_4$. Scan rate: ν = 0.01V.

Table 1. Effect of the storage time without use in the supporting electrolyte solution on the voltammetric charge of a POAP film.

[a]POAP films	[b] Storage time/h	[c]$Q_{Red,c}$/mCcm^{-2}	[d]θ_c[d]
1	32	2.65	0.05
2	45	2.52	0.10
3	52	2.37	0.15
4	60	2.10	0.25
5	72	1.83	0.35
6	83	1.67	0.41
7	96	1.12	0.62
8	120	0.62	0.77

[a] Numbers 1 to 8 represent different deactivated POAP films.

[b] Storage time (in hours) of each POAP film in the supporting electrolyte solution.

[c] Voltammetric reduction charge of the different deactivated POAP films after being held without use in the supporting electrolyte solution for the time periods listed in column 2.

[d] Degree of deactivation of each one of the POAP films after being held without use in the supporting electrolyte solution for the time periods listed in column 2. The degree of deactivation achieved by each film after storage was calculated from $\theta c^d = 1- (Q_{Red,c}/Q_{Red,T})$, where $Q_{Red,T}$ (= 2.8 mC cm^{-2}) is the voltammetric reduction charge of a nondeactivated film.

3. ROTATING DISC ELECTRODE VOLTAMMETRY AND *AC* IMPEDANCE MEASUREMENTS IN THE PRESENCE OF AN ELECTROACTIVE SOLUTION

RDEV and EIS experiments were also performed to study the POAP deactivation with STWU for long time periods. In this regard, steady-state current-potential curves in the presence of the hydroquinone/*p*-benzoquinone redox couple were recorded at different electrode rotation rates, Ω, for both nondeactivated (Fig. **2A**) and deactivated films (Fig. **2B**) [8]. Only the electrochemical behavior of nondeactivated and deactivated POAP films at negative potential values (E < 0.0 V) was considered in our work. Limiting currents at potential values lower than E = 0.0 V were interpreted on the basis of the traditional electron hopping model [9-11].

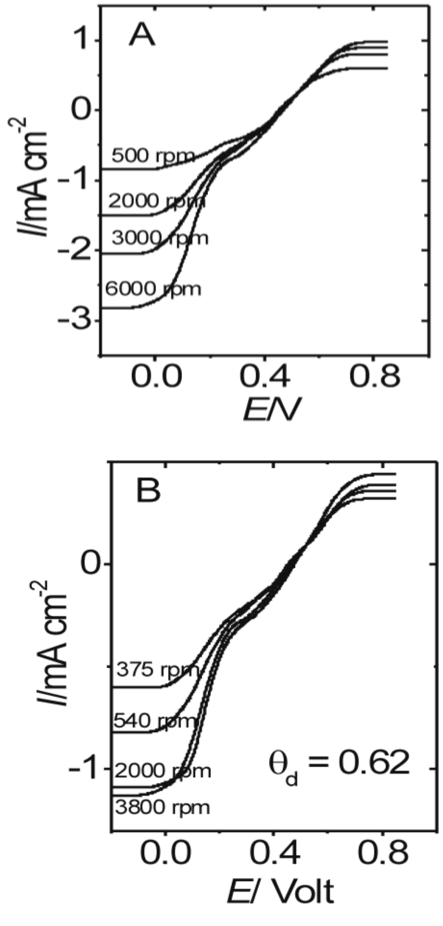

Fig. (2). Steady-state current-potential (I-E) curves for different rotation rates (Ω) of the rotating disc electrode. (A) A nondeactivated POAP film. (B) A deactivated film (θ_d = 0.62). Ω Values are indicated in the figure. Film thickness: 60 nm. Electrolyte: 0.1 M $HClO_4$ + 0.4 M $NaClO_4$+ 2 x 10^{-3} M(HQ/Q).

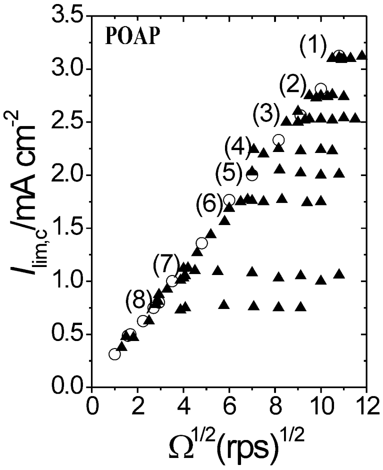

Fig. (3). Levich representations $I_{lim,c}$ *versus* $\Omega^{½}$ for POAP films contacting a 0.1 M $HClO_4$ + 0.4 M $NaClO_4$.+ 2 x 10^{-3} M (HQ/Q) solution. (O) Empty circles correspond to a nondeactivated POAP film. Black triangles correspond to deactivated films. Numbers from (1) to (8) indicate the different films listed in Table **1**.

The anodic and cathodic limiting current at each Ω value for a deactivated POAP film is lower than that for a nondeactivated one (Fig. **2A** and **B**). Also, after a given electrode rotation rate, which depends on the degree of deactivation, the cathodic limiting current for a deactivated film becomes independent of Ω. Fig. **3** compares $I_{lim,c}$ *versus* $\Omega^{1/2}$ dependences for both nondeactivated and deactivated POAP films. For a nondeactivated POAP film, $I_{lim,c}$ *versus* $\Omega^{1/2}$ dependence follows the Levich equation. Limiting current values at which $I_{lim,c}$ (= I_e) becomes constant were considered as a representation of the maximum flux of electrons confined in the polymer, according to Eq. (2) [11]

$$I_e = n\,F\,A\,D_e\,c/\phi_p \qquad (2)$$

In Eq. (2), c is the concentration of redox sites of the polymer and ϕ_p the polymer film thickness. D_e represents a measure of the electron hopping rate and n expresses the numbers (fractions) of unit charges per monomer unit of the polymer. A is the electrode area and F the Faraday's constant. Experimental limiting I_e values, corresponding to each one of the deactivated POAP films indicated in Table **1** were extracted and D_e as a function of the degree of deactivation was obtained from Eq. (2) (Fig. **4**). As can be seen, a linear D_e decrease is observed as θ_d increases The electron diffusion coefficient, D_e, in electroactive materials has been expressed as D_e = (a^2k_o), where k_o is the intermolecular electron-transfer rate constant and a is the mean distance between two adjacent redox sites [12]. The hopping rate, k_o, exhibits an exponential dependence on a. The decrease of D_e was attributed to an increase of the hopping distance between remnant active redox sites after polymer deactivation by storage.

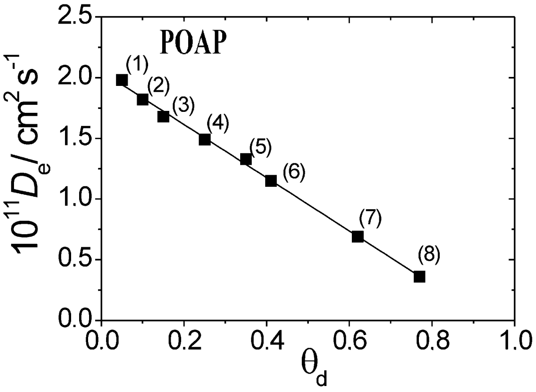

Fig. (4). Electron diffusion coefficient (D_e) (Eq. (2)) as a function of θ_d. Numbers (1) to (8) correspond to each one of the deactivated POAP films listed in Table **1**.

Ac impedance diagrams were also recorded at potential values E < 0.0 V (SCE) for both nondeactivated and deactivated POAP films contacting a 0.1 M $HClO_4$ + 0.4 M $NaClO_4$ + 2 x 10^{-3} M (Q/HQ) solution. Nyquist diagrams at different electrode rotation rates for a nondeactivated POAP film and a deactivated film are shown in Fig. **5A** and **B**, respectively. A Warburg region at high frequency, followed by a semicircle, is observed in the impedance diagrams of a nondeactivated film. Impedance diagrams of deactivated POAP films exhibit two loops. In this regard, at a given Ω value, the higher the θ_d value, the greater the high-frequency semicircle.

The general theory of *ac* impedance described by Vorotyntsev *et al.* in [13] was employed to interpret experimental impedance data of nondeactivated and deactivated POAP films. As in the present case, one has the modified electrode geometry with a redox active electrolyte solution (m|film|es), Eq. (41) of Ref. [13] (Eq. (3) in this work) must be applied

$$Z_{m|film|es} = R_{m|f} + R_f + R_s + [Z_e^{f|s}\,R_i^{f|s} + W_f\,Z_{12}^{m}]\,(Z_e^{f|s} + R_i^{f|s} + 2\,W_f \coth 2\nu)^{-1} \qquad (3)$$

where

$$Z_{12}^{m} = Z_e^{f|s}\,[\coth\,\nu + (t_e - t_i)^2 \tanh\,\nu] + R_i^{f|s}\,4t_i^2 \tanh\,\nu + W_f\,4t_i^2 \qquad (4)$$

In Eqs. (3) and (4):

$\nu = [(j\omega\phi_p^2)/4D]^{1/2}$ is a dimensionless function of the frequency ω, ϕ_p is the film thickness, D is the binary electron-ion diffusion coefficient, and t_i and t_e are the migration (high frequency) bulk-film transference numbers for anions and electrons, respectively. D is defined as $D = 2D_iD_e(D_e+D_i)^{-1}$ and $t_{i,e} = D_{i,e}(D_e+D_i)^{-1}$, where D_e and D_i are the diffusion coefficients for the electrons and ion species, respectively.

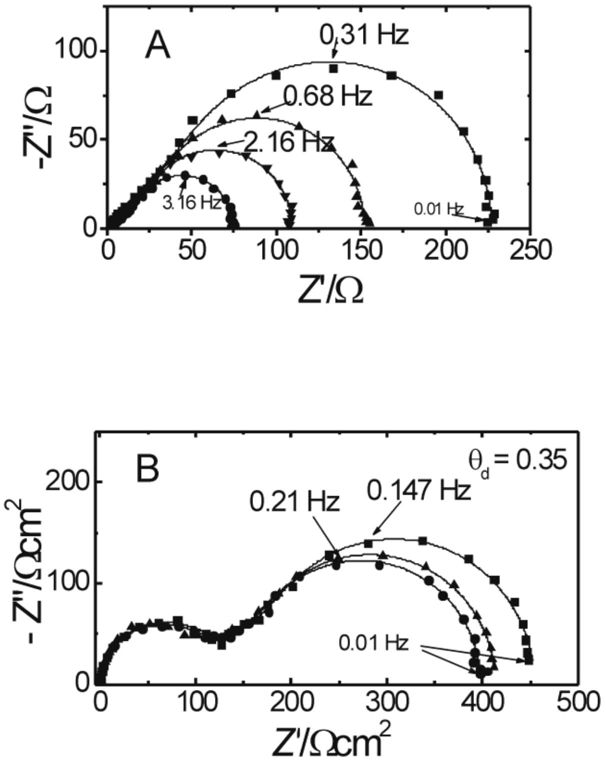

Fig. (5). *Ac* impedance diagrams in the Nyquist coordinates (-*Z*" *versus Z*) obtained at *E* = -0.3 V for (A) a nondeactivated POAP film and (B) for a deactivated film. The different diagrams correspond to different electrode rotation rates, Ω: (■) 100 rpm; (▲) 200 rpm; (▼) 300 rpm; (●) 600 rpm. Electrolyte: 0.1 M $HClO_4$ + 0.4 M $NaClO_4$ + 2 x 10^{-3} M (HQ/Q) solution.

$W_f = [\nu/j\omega\phi_pC_p] = \Delta R_f/\nu$ is a Warburg impedance for the electron-ion transport inside the polymer film. ΔR_f $(=\phi_p/4DC_p)$ is the amplitude of the Warburg impedance inside the film, and C_p is the redox capacitance per unit volume.

R_f $(=\phi_p/\kappa)$ is the high-frequency bulk-film resistance, R_s the ohmic resistance of the bulk solution (κ is the high-frequency bulk conductivity of the film), $R_{m|f}$ is the metal|film interfacial electron-transfer resistance, and $R_i^{f|s}$ is the film|solution interfacial ion-transfer resistance.

$Z_e^{f|s} = (R_e^{f|s}+W_s)$ is the electronic impedance, where $R_e^{f|s}$ is the interfacial electron-transfer resistance at the film|solution interface, and W_s is the convective diffusion impedance of redox species in solution, which contains the bulk concentrations of ox(red) forms, $c_{ox}(c_{red})$, and their diffusion coefficients inside the solution, $D_{ox}(D_{red})$. Also, it contains the Nernst layer thickness, δ.

$R_e^{f|s}$ is defined as

$$R_e^{f|s} = RT\,(nF^2k_oc_{red})^{-1} \qquad (5)$$

where k_o is the rate constant of the reaction between the film and the redox active forms in solution. Diffusion of the redox forms from the bulk solution to the film|solution interface can be regarded as stationary through the diffusion layer thickness, expressed in cm by

$$\delta = 4.98\,D_{ox,red}^{1/3}\,\eta^{1/6}\,\Omega^{-1/2} \qquad (6)$$

where η is the kinematic viscosity of the solution in the same units as $D_{ox,red}$, and Ω the rotation rate of the disk electrode in rpm. The rest of the constants have their usual meaning. The fitting of

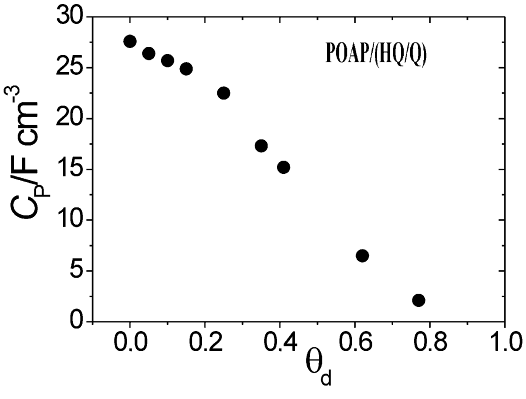

Fig. (6). Redox capacitance (C_p) as a function of θ_d. The value 27.5 F cm^{-3} for θ_d = 0 corresponds to a nondeactivated film.

experimental data using Eq. (3) allows one to obtain the dependencies of the different charge-transport and charge-transfer parameters on the degree of deactivation.

The C_p versus θ_c dependence is shown in Fig. **6**. A break at a degree of deactivation about 0.3 is observed.

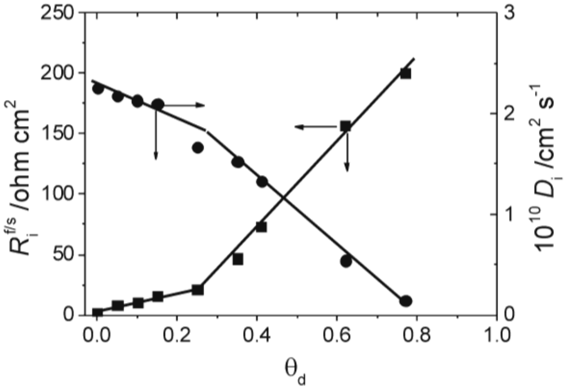

Fig. (7). Polymer-solution interfacial ion-transfer resistance ($R_i^{f/s}$) and ion diffusion coefficient (D_i) as a function of θ_d.

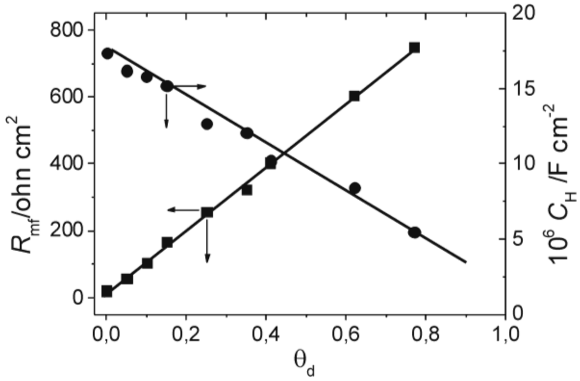

Fig. (8). Metal-polymer interfacial electron-transfer resistance ($R_{m/f}$) and interfacial capacitance C_H at the metal-polymer interface as a function of θ_d.

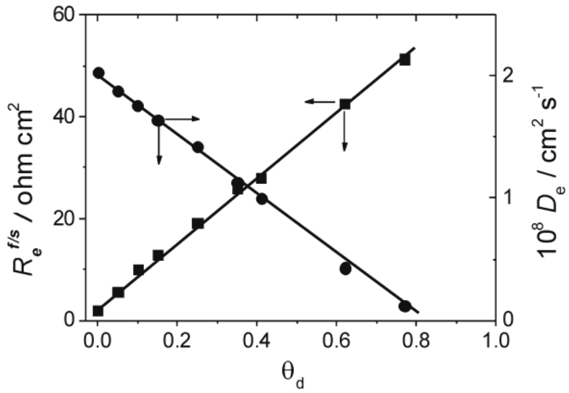

Fig. (9). Interfacial electron-transfer resistance ($R_e^{f/s}$) and electron diffusion coefficient (D_e) as a function of θ_d.

As can be seen from Fig. **7**, both $R_i^{f|s}$ and D_i show a clear break about a degree of deactivation of 0.3. The $R_i^{f|s}$ increase with the increase of the degree of deactivation could be attributed to an increasing difficulty to incorporate ions across the polymer/solution interface into the polymer matrix as the polymer becomes more deactivated. Also the D_i decreases could be related to an increasing difficulty to transport ions into the polymer as it becomes more deactivated. Fig. **8** shows the increase of interfacial $R_{m|f}$ resistance and the decrease of C_H with the θ_d increase. Both the effects could be due to an increasing number of inactive sites at the metal|polymer interface with the increase of deactivation. Also, the increasing number of inactive sites affects $R_e^{f|s}$ and D_e vs. θ_d dependencies (Fig. **9**). It is interesting to notice that while some parameters as D_e decrease almost linearly with the increase of θ_d, other ones such as, D_i and $R_i^{f|s}$ show a break at a given degree of deactivation (θ_d = 0.3). It is possible that both parameters $R_i^{f|s}$ and D_i are related to proton movements across the POAP|solution interface and inside the polymer film, respectively, rather than to anion transport.The existence of two types of protons at POAP has been proposed [14]. The C_H decrease and the $R_{m|f}$ increase could be assigned to the creation of inactive gaps in the redox site configuration at the polymer|metal interface with deactivation. It is interesting to notice that similar charge-transport and charge-transfer parameter changes are observed for the deactivation of other electroactive materials, such as, nickel hydroxide [15].

3. SURFACE RESISTANCE MEASUREMENTS

In previous works it was proved that SR is a useful technique to detect changes in the redox sites distribution during the redox switching of a POAP film deposited on a thin gold film [16]. Usually, the relative resistance change as a function of potential (*ΔR/R-E*) is recorded in SR experiments, where *R* is the initial resistance value of the gold film and depends on the film thickness. Eight gold film electrodes were synthesized [17] and then they were coated with a 60 nm POAP film. These POAP coated gold film electrodes were consecutively subjected to the different storage times listed in Table **1** and then, the *ΔR/R-E* responses were recorded (Fig. **10**).

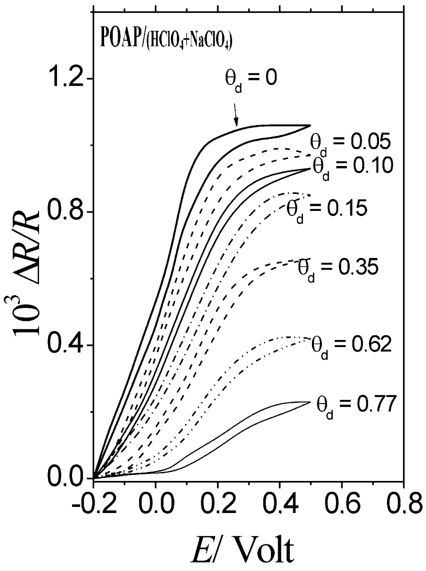

Fig. (10). *ΔR/R-E* responses of POAP coated gold film electrodes subjected to different STWU. The degrees of deactivation are indicated in the figure. Thickness of the gold film ϕ_m = 30 nm, resistance value of the gold film, *R* = 20.02 ohm. Thickness of the POAP film, ϕ_P = 60 nm. Electrolyte: 0.1 M $HClO_4$ + 0.4 M $NaClO_4$. Scan rate: $\nu = 0.01 V s^{-1}$.

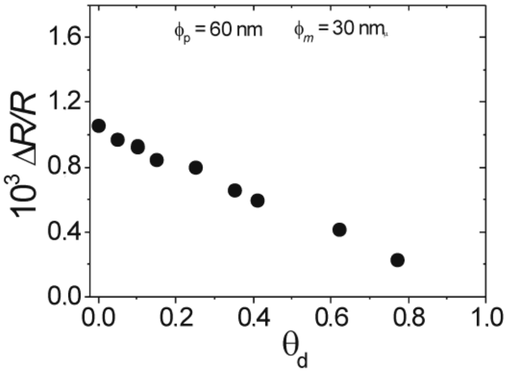

Fig. (11). Maximum *ΔR/R* change in going from the reduced to the oxidized state of POAP as a function of the degree of degradation, θ_d. Thickness of the POAP film, ϕ_P = 60 nm. Thickness of the gold film, ϕ_m: 30 nm.

The conversion of amine to imine sites occurs during the transition from the reduced to the oxidized state of POAP [18]. The increase of *ΔR/R* during POAP oxidation can be explained in terms of an interfacial distribution of scatterers (imine sites) in the oxidised state with a spacing among them larger than that corresponding to amine sites in the reduced state [16,18]. That is, the distribution of imine species in the oxidized state of POAP should be less compact than the corresponding distribution of amine species in the reduced state, which should lead to a more diffuse reflection of conduction electrons at the gold|POAP interface. In this respect, optical measurements on POAP films reveal that only one in every four or five amine sites is converted to the corresponding imine site [18]. Thus, the existence of inactive gaps within the distribution of oxidized sites of POAP could justify that POAP in its oxidized state reflects conduction electrons of gold more diffusely than in its reduced state. Fig. **10** shows the attenuation in the *ΔR/R* response in going from the reduced to the oxidized state of POAP as θ_d increases (Fig. **10**). The *ΔR/R* value at *E* = 0.5 V (SCE) decreases linearly with the θ_d increases (Fig. **11**). This effect can be attributed to a lower amount of scattering centers (imine sites) for the diffuse reflection of conduction electrons as θ_d increases. At this point a comparison between $R_{m|f}$ and *ΔR/R* changes with the degree of deactivation (Figs. **8** and **11**, respectively) can be established. While the increase of $R_{m|f}$ during the deactivation of the polymer film should be associated with a transversal resistance due to the electron transfer across the polymer/metal interface, the *ΔR/R* decrease with POAP deactivation can be attributed to the scattering of conduction electrons from the inside of the metal to the metal/polymer interface, caused by changes in the translational symmetry parallel to the interface due to the presence of a different distributions of redox sites at the interface. Despite both resistances being associated to the redox sites distribution at the metal/POAP interface, it should be taken into account that the while *ΔR/R* change (-0.2 V to 0.5 V) is obtained from a potentiodynamic technique (CV), $R_{m|f}$ is extracted at the reduced state of POAP employing EIE. Moreover, while the increase of $R_{m|f}$ should be associated to an increase of the amount of inactive redox sites at the reduced state during POAP deactivation, the *ΔR/R* decrease could be attributed to the change of the reflecting properties of the redox sites distributions at the reduced and oxidized states of POAP for the conduction electrons of the gold film which tend to match as the polymer becomes more deactivated.

CONCLUSION

Poly(o-aminophenol) films maintain their conducting properties unaltered even after a storage time without the use of one day. However, a loss of conductivity was observed as the storage time was extended beyond 30 h. An attenuation of the voltammetric response of POAP is observed with the increase of the storage time. The electron hopping model was employed to interpret RDEV experiments. EIS data were interpreted on the basis of a model which allows one to explain both ionic and electronic interfacial exchange across the POAP/solution interface. While electron (D_e) and ion (D_i) diffusion coefficients decrease, interfacial resistances ($R_{m|f}$, $R_i^{f|s}$, $R_e^{f|s}$) increase as the degree of deactivation of the polymer increases. The slower electron transport with the increase in the degree of deactivation was attributed to the increase of the electron hopping distance between redox sites, While parameters representing electron motion extracted from RDEV and impedance measurements seem to change continuously within the whole range of deactivation degree, parameters representing the ion transport show a break at a degree of deactivation of about 0.35. This characteristic of the ion transport at POAP was associated with the existence of two forms of hydrogen ions in the POAP film. The relative surface resistance change of a thin gold film coated with poly(*o*-aminophenol) is gradually attenuated with the increase of the storage time. The attenuation of the surface resistance change as the degree of deactivation of POAP increases was attributed to a lower amount of active redox sites which act as scattering centers for the conduction electrons.

CONFLICT OF INTEREST

The authors declare no conflict of interest, financial or otherwise.

ACKNOWLEDGEMENTS

The author gratefully acknowledges the Consejo Nacional de Investigaciones Científicas y Técnicas (CONICET) and also the Facultad de Ciencias Exactas, National University of La Plata (UNLP).

REFERENCES

[1] Miras, M.C.; Badano, A.; Bruno, M.M.; Barbero, C. Nitric oxide electrochemical sensors based on hybrid films of conducting polymers and metal phtalocyanines. *Portugaliae Electrochimica Acta*, **2003**, 21, 235-243.

[2] Yano, J.; Kawakami, H.; Yamasaki, S.; Kanno, Y. Cation capture ability and the potential response of a poly(*o*-aminophenol) film electrode to dissolved ferric ions. *J. Electrochem. Soc.*, **2001**, 148, E61-E65.

[3] Lobo, M.J.; Miranda, A.J.; López-Fonseca, J.M.; Tuñón, P. Electrocatalytic detection of nicotinamide coenzymes by poly(*o*-aminophenol) and poly(*o*-phenylenediamine)-modified carbon paste electrode. *Analytica Chimica Acta*, **1996**, 325, 33-42.

[4] Zhang, A.Q.; Cui, C.Q.; Lee, J.Y. Metal-polymer interaction in the Ag^+/poly-*o*-aminophenol system. *J. Electroanal. Chem.*, **1996**, 413, 143-151.

[5] Tucceri, R. Redox transformation of poly(o-aminophenol) (POAP) film electrodes under continuous potential cycling, *Procedia Materials Science*, **2015**, 8, 261-270.

[6] Tucceri, R. Deactivation of poly(o-aminophenol) film electrodes by storage without use in the supporting electrolyte solution and its comparison with other deactivation processes. A study employing EIE, *Journal of Applied Electrochemistry*, **2015**, 45, 1123-1132.

[7] Tucceri, R. Charge-transfer and charge-transport parameters of deactivated poly(o-aminophenol) film electrodes. A study employing electrochemical impedance spectroscopy, *J. Electroanal. Chem.*, **2011**, 659, 1, 83-91.

[8] Bonfranceschi, A.; Pérez Córdoba, A.; Keunchkarian, S.; Zapata, S.; Tucceri, R. Transport across poly(*o*-aminophenol) modified electrodes in contact with media containing redox active couples. A study using rotating disc electrode voltammetry. *J. Electroanal. Chem.*, **1999**, 477, 1-13.

[9] Andrieux, C.P.; Savéant, J.M. Electron transfer through redox polymers films. *J. Electroanal. Chem.*, **1980**, 111, 377-381.

[10] Laviron, E. A multilayer model for the study of spaced distribute redox modified electrodes. Part 1. Description and discussion of the model. *J. Electroanal. Chem.*, **1980**, 112, 1-9.

[11] Deslouis, C.; Tribollet, B. Hydrodynamic impedance. In: *Advances in Electrochemical Science and Engineering*; Gerischer, H.; Tobias, C., Eds. VCH Publishers, New York, USA, **1992**; vol. 2, pp. 205.

[12] Chidsey, Ch.E.D.; Murray, R.W. Redox capacity and direct current electron conductivity in electroactive materials. *J. Phys. Chem.*, **1986**, 90, 1479-1484.

[13] Vorotyntsev, M.A.; Deslouis, C.; Musiani, M.M.; Tribollet, B.; Aoki, K. Transport across an electroactive polymer film in contact with media allowing both ionic and electronic interfacial exchange. *Electrochim. Acta*, **1999**, 44, 2105-2115.

[14] Levin, O.; Kondratiev, V.; Malev, V. Charge transfer processes at poly-*o*-phenylenediamine and poly-o-aminophenol films. *Electrochim. Acta*., **2005**, 50, 1573-1585.

[15] Tucceri, Ricardo, A study of the charge transport process at nickel hydroxide-gold modified electrodes employing rotating disc electrode voltammetry and ac impedance spectroscopy, *Sop Transactions on Physical Chemistry*, **2014**, 1, 33-44.

[16] Tucceri, R. A review about the surface resistance technique in electrochemistry. *Surface Science Reports*, **2004**, 56, 85-157.

[17] Tucceri, R. Deactivation of poly(o-aminophenol) film electrodes by storage without use in the supporting electrolyte solution and its comparison with other deactivation processes, *J. Electroanal. Chem.*, **2015**, 739, 58-65.

[18] Tucceri, R.I.; Barbero, C.; Silber, J.J.; Sereno, L.; Posadas, D. Spectroelectrochemical Study of Poly(*o*-aminophenol). *Electrochim. Acta*, **1997**, 42, 919-927.